

Introduction to Induction Machines and Power Electronics

J. McCalley

1.0 Overview

In these notes, we will introduce two important areas of electrical engineering, power electronics and induction machines, and then we will combine these two areas to study a third, doubly fed induction generators (DFIGs).

Power electronic circuits are used in many different applications, but perhaps the most ubiquitous of these is the speed control of electric motors. The most common electric motor is the induction motor, which can be thought of as the workhorse of manufacturing. An area which puts both power electronics and induction machines together, and that has become highly important in the world today, especially in Iowa, is wind energy.

Figure 1 illustrates the basic configurations associated with wind turbines today. We observe that the configurations on the right-hand-side both contain power electronic converters. The configuration at the top right, the DFIG, represents the most common type of wind turbine installed today. The configuration on the bottom right represents what most people believe to be poised to gain significant market share in the future. Both configurations on the left represent designs that were initially used quite heavily, and as a result, are found in the field quite a bit; however, very few new turbines use them today.

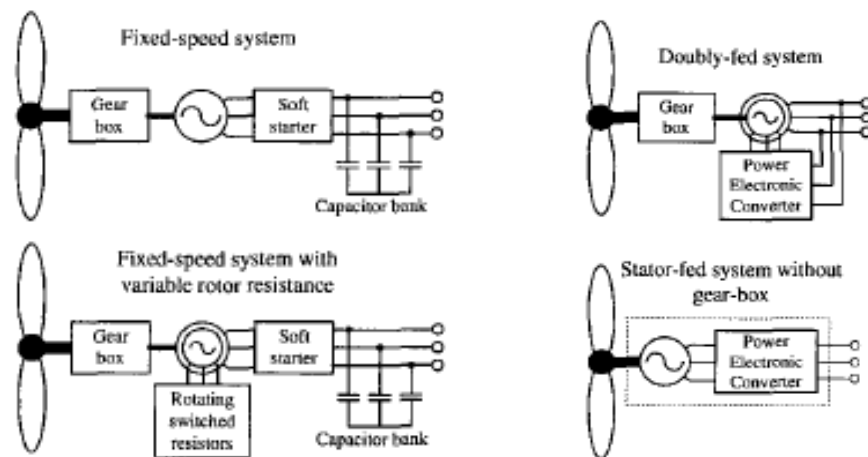


Fig. 1 [1]

Because the DFIG is commonly found in the field today, and because it is likely to continue to be a configuration used in new turbines, we will build the necessary fundamentals in this class to understand how it operates. To complement this material, you should reread Section 6.2 in your text [2] which provides an overview of wind energy, Chapter 10 on power electronics, and Section 12.2 on induction machines.

2.0 Squirrel-Cage Induction Generators

We recall that the speed-torque (or slip-torque) relation for a squirrel-cage induction machine is given by

$$T = \frac{3V_{th}^2 R_2'}{(s\Omega_s) \left[\left(R_{th} + \frac{R_2'}{s} \right)^2 + (X_{th} + X_2')^2 \right]} \quad (1)$$

where Ω_s is the synchronous speed of the machine given by $120f/p$ (f is frequency and p is number of poles), R_2' and X_2' are the rotor resistance and leakage reactance, respectively, V_{th} and $Z_{th}=R_{th}+jX_{th}$ are the Thevenin voltage and impedance, respectively, seen looking into the stator part of the equivalent circuit from the rotor, as illustrated in Fig. 2, and the slip s is given by

$$s = \frac{(\Omega_s - \Omega_m)}{\Omega_s} \quad (2)$$

We will work an example to explore the speed-torque relation.

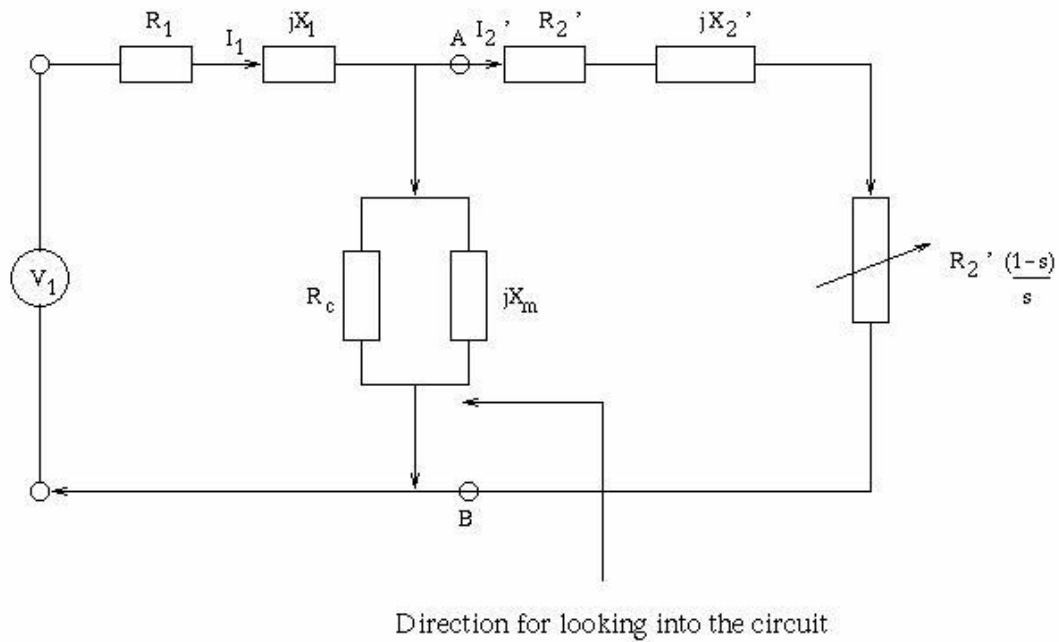


Fig. 2

Example: Consider a 6-pole induction generator with line-line voltage of 220 volts, and the below data. Plot the torque-speed characteristic for $f=60$ Hz.

$$\begin{aligned}
 R_1 &= 0.294 \, \Omega & X'_2 &= 0.209 \, \Omega \\
 X_1 &= 0.503 \, \Omega & R'_2 &= 0.061 \, \Omega \\
 R_c &= 1000 \, \Omega \\
 X_m &= 13.25 \, \Omega
 \end{aligned}$$

Solution: First we need to obtain Ω_s . This is given by

$$\Omega_s = 2\pi f / (p/2) = 2\pi(60) / (6/2) = 125.664 \text{ rad/sec}$$

This should be denoted Ω_s here and then likewise in the below matlab script.

We develop the speed-torque characteristic using the following Matlab code.

```

v1= 220/sqrt(3);
r1=0.294;
x1=0.503;
rc= 1000;
xm=13.25;
xp2=0.209;
rp2=0.0610;
ws=125.67;
% Compute thevenin
parameters.
zb=(rc*i*xm)/(rc+i*xm);
za=r1+i*x1;
vth=abs(v1*zb/(za+zb));
zth=za*zb/(za+zb);

```

```

rth=real(zth);
xth=imag(zth);
% Mechanical speed range
wm1=[0*k*ws:1:2*k*ws];
% Torque equation components.
num=3*(vth^2)*rp2;
den1=ws*(1-wm1/(k*ws));
den2=(rth+rp2./(1-wm1/(k*ws))).^2;
den3=(xth+xp2)^2;
% Compute torque
T1=num ./ (den1.*(den2+den3));
plot(wm1,T1)
grid

```

The above Matlab code results in the speed-torque relationship shown in Fig. 3. We observe here that

- Motor operation is from $\Omega_m=0$ to $\Omega_m= \Omega_s=125.664$ rad/sec; reference to (1) shows this corresponds to positive slip.
- Generator operation is from $\Omega_m=\Omega_s=125.664$ rad/sec to $\Omega_m=2\omega_s=251.328$ rad/sec; reference to (1) shows this corresponds to negative slip.
- The developed torque for motor operation is positive and for generator operation is negative.
- The maximum developed torque for motor operation is about half of the maximum developed torque for generator operation. The reason for this can be seen in eq. (1) where the slip, when negative (generator operation), results in a torque expression denominator that is smaller than when the slip is positive (motor operation).

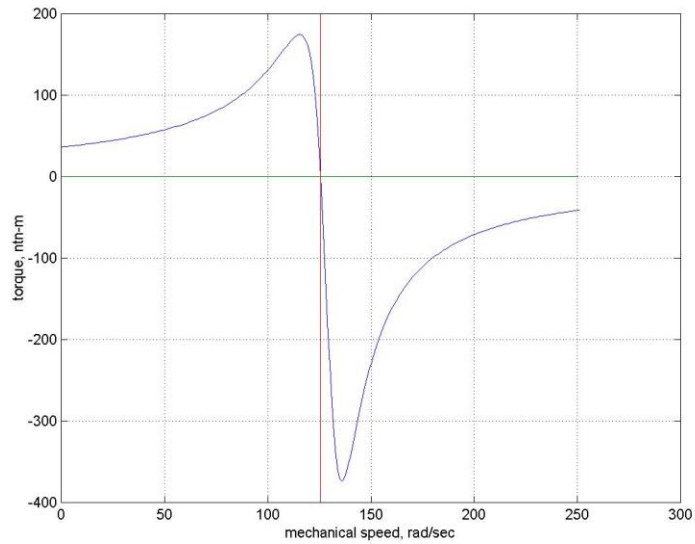


Fig. 3

Now let's consider a situation where our induction machine, with its stator windings connected to a 60 Hz electric power grid, is operating as a motor while driving a wind turbine through a gear box, as shown in Fig. 4 [3].

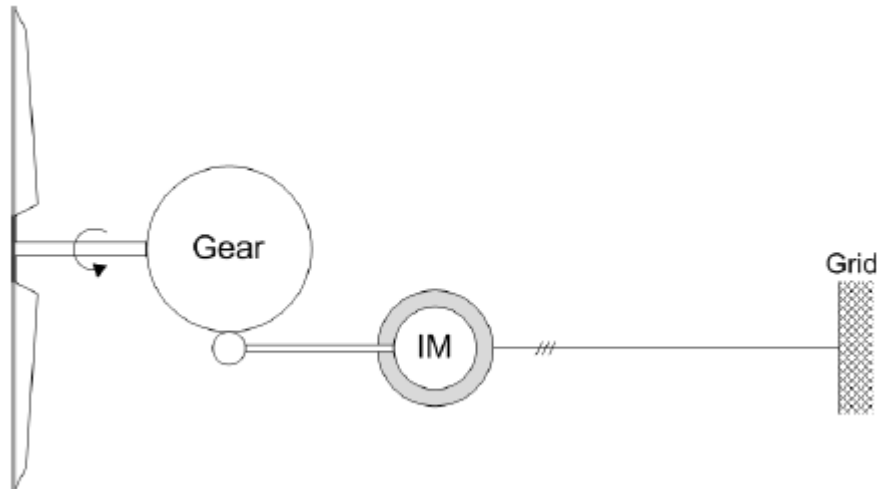


Fig. 4 [3]

We assume that the induction machine phases are connected to the grid so that the rotating magnetic field from the stator currents exert torque on the rotor and the wind turbine is rotated (through the gear box) by the electromagnetic torque exerted on the rotor. This situation is essentially equivalent to an induction motor driving a very large fan! There is an equal and opposite mechanical torque exerted by the "fan" (wind turbine), as illustrated in Fig. 5.

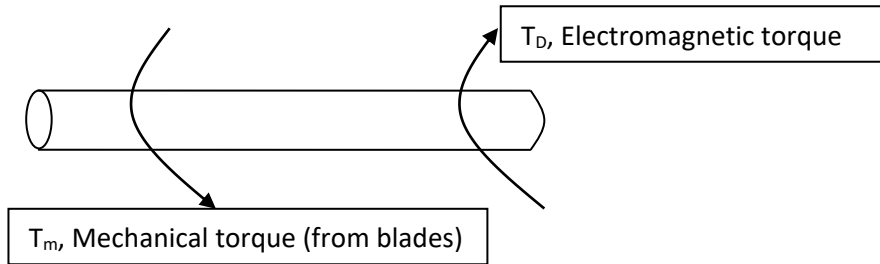


Fig. 5

Let's assume that the speed-torque characteristic of the "fan" is as in Fig. 6, which means that the equilibrium point (the steady-state operating point) is the intersection of the two speed-torque characteristics.

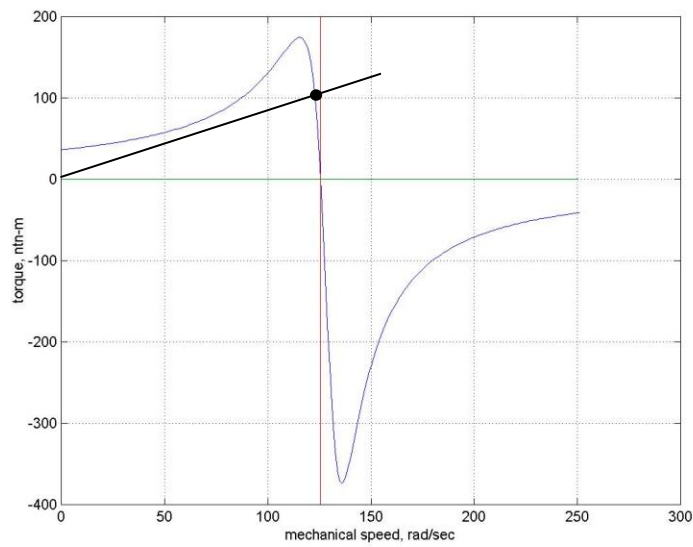


Fig. 6

Now let's assume that the wind picks up speed, exerting torque on the blades in the same direction that it is rotating (but in opposite direction to that of the mechanical torque illustrated in Fig. 5). The rotor will increase its speed in response to this mechanical torque, and when that speed equals synchronous speed (in our example, $\Omega_s=125.664$ rad/sec), the electromagnetic torque of the machine is 0. As the speed is further increased, the electromagnetic torque goes negative. At this point, the directionalities of the torques are as shown in Fig. 7.

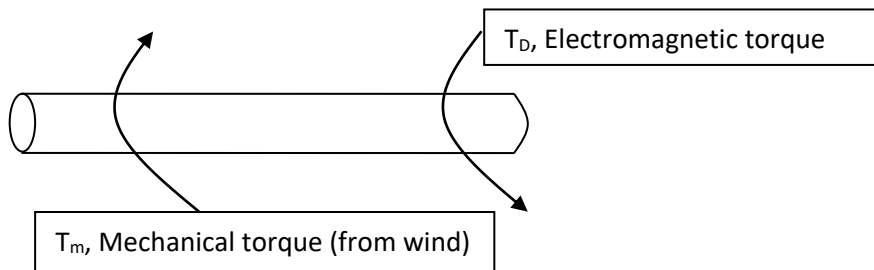


Fig. 7

Torque-speed characteristics associated with wind turbines are not simply a function of a mechanical load but also reflect the aerodynamic features of the wind-blade interaction, and as a result, appear as shown in Fig. 8, where the numbers 4-10 correspond to wind speed (m/sec). We observe that as the wind speed increases, the electromagnetic torque increases significantly, but the speed of the machine changes very little. For this reason, this kind of wind turbine configuration, using an induction machine with a squirrel cage rotor, is referred to as a fixed-speed machine.

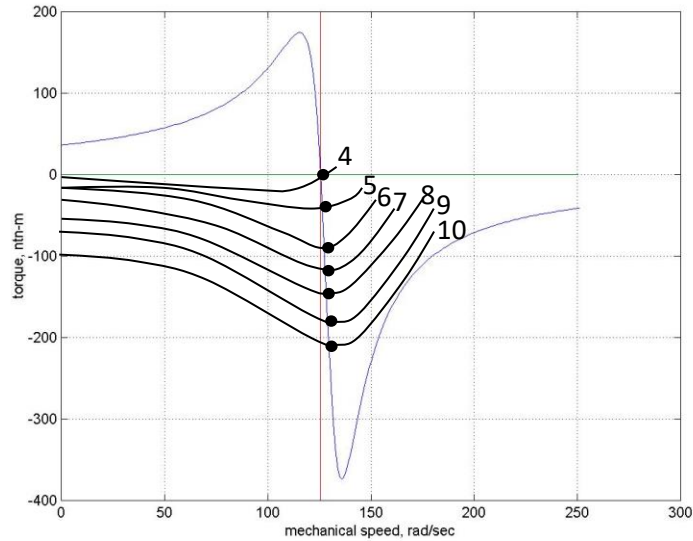


Fig. 8

Fix-speed machines were the first type of wind turbines used, and there are still a large number of them in operation today. However, they incur a significant problem in that the output torque (and the output power given almost constant speed and that $P=T\omega_m$), fluctuates with the wind speed. Since wind speed can vary significantly in a short-amount of time, fixed speed wind turbines tend to cause large power variations in the grid which increase the grid's need to perform regulation, a problem referred to as wind-gusts. In addition, fixed-speed machines do not have the ability to adjust turbine speed as a function of wind speed and thus enable the aerodynamic rotor to operate at its maximum efficiency over a wide range of wind speeds. There have been several wind-speed configurations developed to overcome these disadvantages, but the most heavily used of these is the doubly-fed induction generator, described in the next section.

3.0 Doubly Fed Induction Generators

The doubly-fed induction generation (DFIG) is illustrated in Fig. 9. The principle of operation for the DFIG is that by controlling the rotor frequency and currents, we may control the rotor speed and the electrical power (real and reactive) output of the machine. This control on speed and electrical power output is considered to be highly refined, in contrast to blade pitch control which enables control of the mechanical power input to the generator.

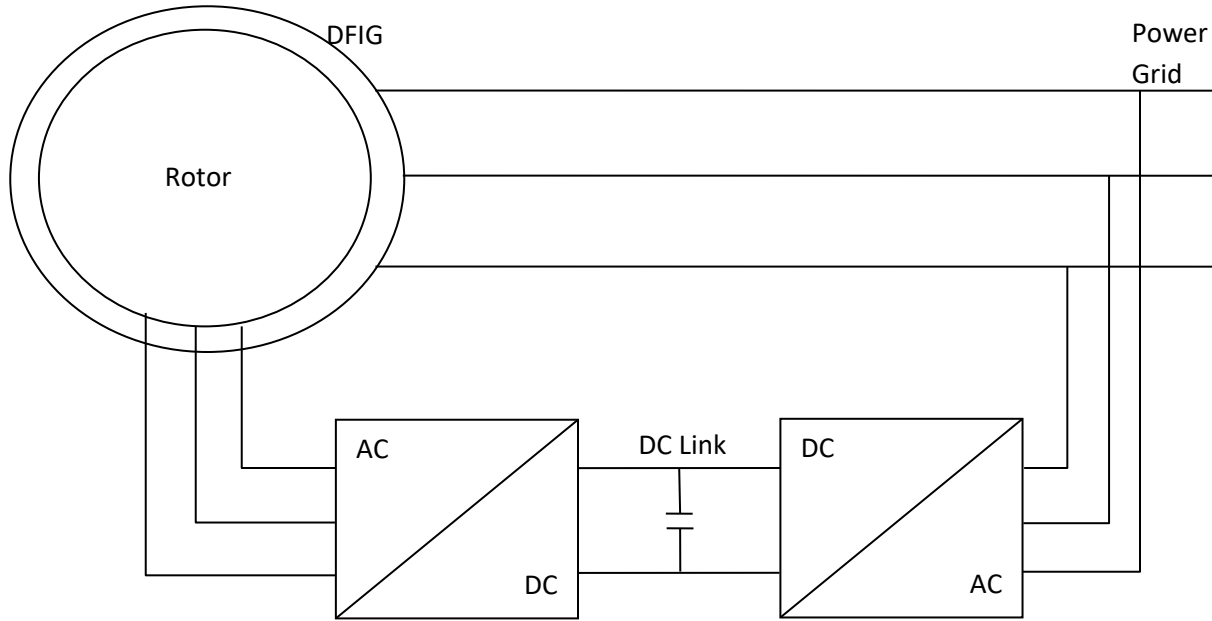


Fig. 9

We will focus on control of DFIG rotor speed. To consider this, recall that the definition of slip is:

$$s = \frac{(\omega_s - \omega_m)}{\omega_s} \quad (3)$$

The difference $\omega_s - \omega_m$ is the relative motion seen by the rotor windings and is therefore the frequency induced in these windings, ω_r . In the subsynchronous mode, when $\omega_s > \omega_m$, then :

$$\omega_r = \omega_s - \omega_m \quad \rightarrow \quad \omega_m = \omega_s - \omega_r \quad (3)$$

In the supersynchronous mode, when $\omega_s < \omega_m$, then, to define frequency as a positive number, we have:

$$\omega_r = \omega_m - \omega_s \quad \rightarrow \quad \omega_m = \omega_s + \omega_r \quad (4)$$

The synchronous speed ω_s is set by the line frequency and therefore must be considered a constant. This means that the mechanical speed of the rotor, ω_m , may be directly controlled by controlling the rotor winding frequency. This is done by inserting a controllable frequency voltage source into the rotor circuit. Figure 10 illustrates.

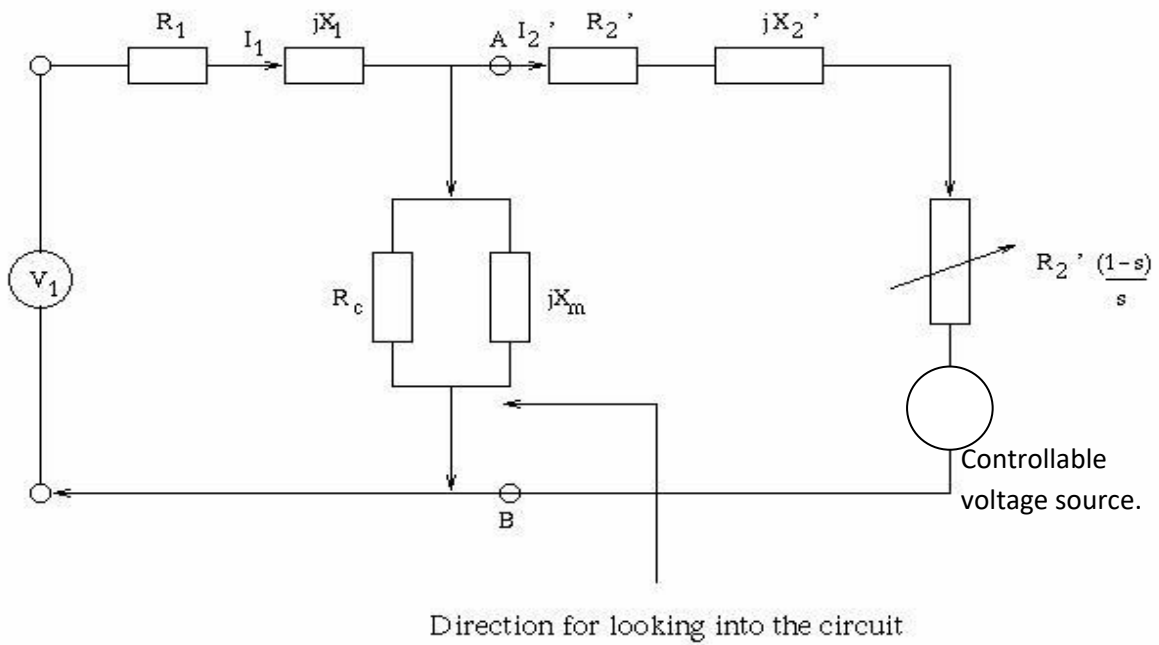


Fig. 10

It is interesting that the DFIG can operate in both the subsynchronous and the supersynchronous mode. Figure 11 below illustrates the flow of power for each of these modes.

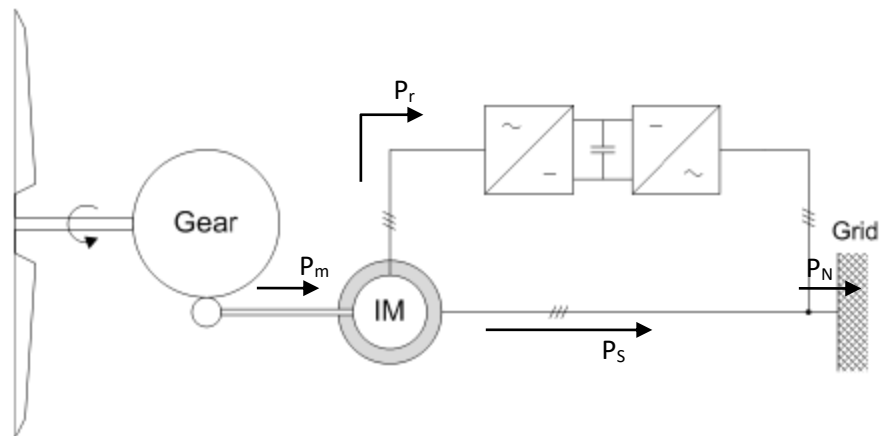


Fig. 11 [3]

In our treatment of the induction motor, we learned that

$$P_m = P_{airgap} (1 - s)$$

(5)

which also holds for the induction generator and the DFIG. If we neglect stator copper losses, then the power crossing the airgap is also the power out of the stator windings P_s . Therefore [4],

$$P_m = P_s (1 - s) \tag{6}$$

A key aspect of an DFIG is its ability to provide power to or absorb power from via the rotor circuit. Reference to Fig. 11 shows that, if we neglect core losses and copper losses in the stator and rotor, then the power into the network P_N is the same as the mechanical power provided to the DFIG, which flows through the stator windings and the rotor windings according to:

$$P_N = P_m = P_s + P_r \tag{7}$$

Finally, it is useful to compare a DFIG wind turbine to a typical steam-driven turbine-generator set, which is done in Fig. 12. Here, the lines from “control” box indicate control capability, not feedback. The steam turbine has 3 types of control available to it: fuel input, steam valve, and generator field, with the first 2 related to speed-power control and the 3rd one related to MVAR-voltage control. In the case of the steam-turbine, the fuel supply controls the input mechanical power, and the steam-valve controls the output mechanical power.

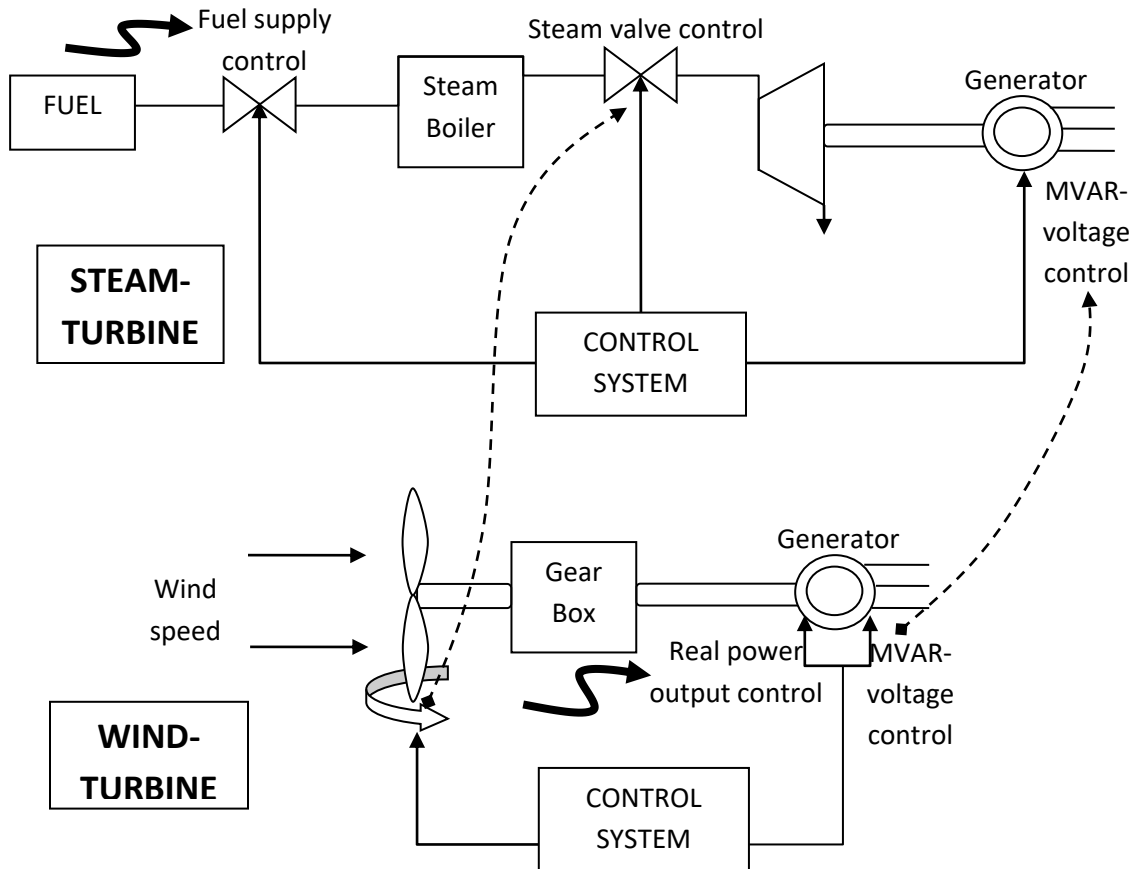


Fig. 12

4.0 Power Electronic Devices

We begin our study by considering power electronic devices. There are many different kinds of such devices, including diodes, thyristors, triacs, metal-oxide field-effect transistors (MOSFETS), bipolar junction transistors (BJTs), and insulated gate bipolar transistors (IGBTs), as summarized in Table 1 [5].

Table 1 [5]

Devices	Symbols	Characteristics
Diode		
Thyristor		
SITH		
GTO		
MCT		
MTO		
ETO		
IGCT		
TRIAC		
LASCR		
NPN BJT		
IGBT		
N-Channel MOSFET		
SIT		

All of them, however, have a common operating behavior when used in power electronic circuits: they are switches! We describe operating characteristics of a few of them in what follows.

4.1 BJT's

You have been introduced to the BJT before in your electronic devices class, where you learned that it has an operating characteristic as shown in Fig. 13.

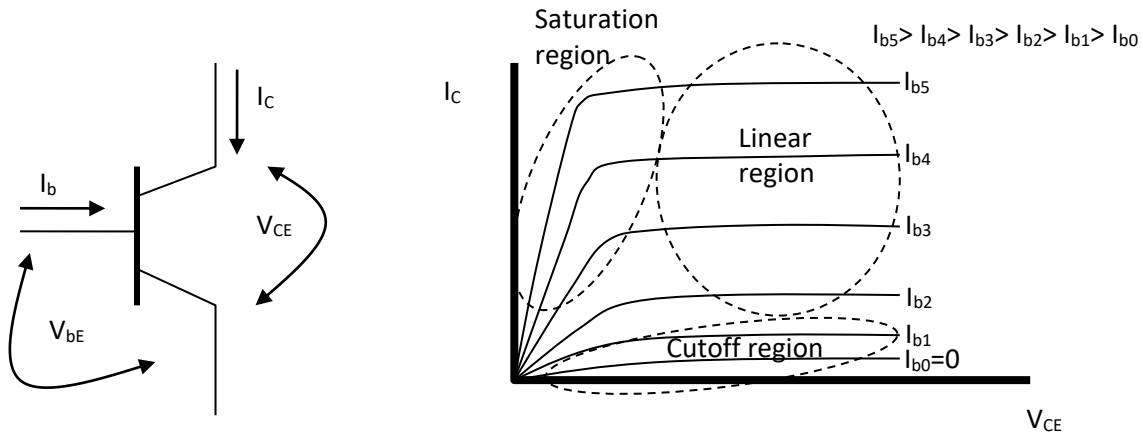


Fig. 13

When BJT's are used in amplifier circuits, they are operated in the linear region where $I_C = \beta I_b$ for an almost constant β .

In power electronic applications, however, we avoid the linear region altogether and simply operate between the other two regions:

- *Cutoff region*: This is achieved by forcing $I_b = 0$. Here, junction C-E looks like an open switch in that for very high V_{CE} , the current I_C remains very small.
- *Saturation region*: This is achieved by forcing I_b to be very high. Here, junction C-E looks like a short circuit in that for very small V_{CE} is, the current I_C is very large. We observe that the device emulates a “normally open” switch, i.e., it is conducting only if the base current is present.

In Fig. 14, the two operating extremes are overlaid on top of an ideal switch characteristic.

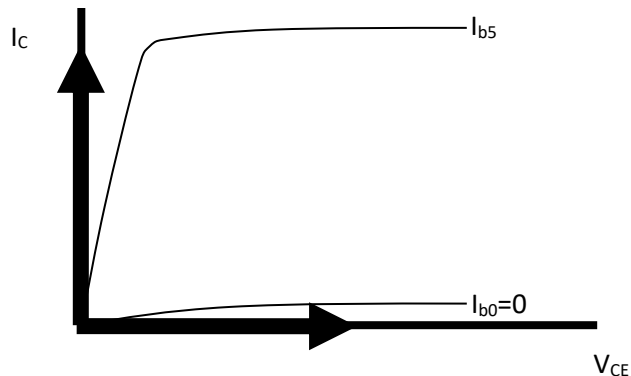


Fig. 14

Aside: Students are often confused about why the “saturation region” of Fig. 2 is so-named. The word “saturation” does not refer to the I_C vs. V_{CE} relationship but rather to the I_C vs. I_b relationship $I_C = \beta I_b$, where β falls off as I_b gets high, as illustrated in Fig. 15.

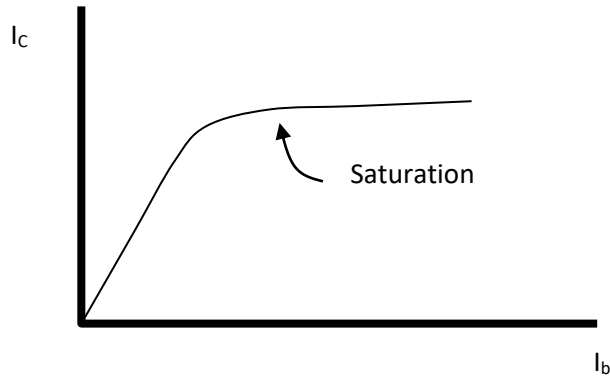


Fig. 15

BJTs have power handling capabilities up to the 1 MW range and switching speeds up to 10 kHz, reasonable in both attributes but not extreme in either.

4.2 MOSFETs

You have also been introduced to Metal Oxide Field Effect Transistors (MOSFETs) in your electronic circuits class, which can be either of the enhancement or the depletion-type. Power MOSFETs are typically of the enhancement type, having V_{gs} always nonnegative. MOSFETs have an operating characteristic as shown in Fig. 16.

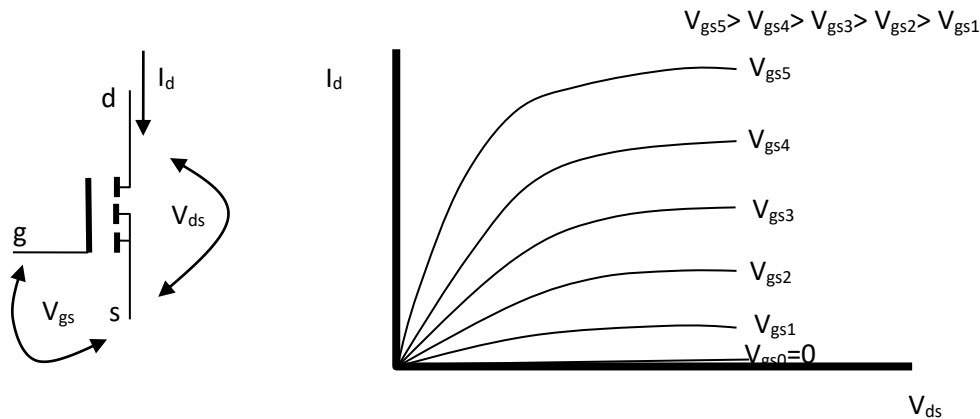


Fig. 16

Like the BJT, the MOSFET will operate like a switch by alternating between

$V_{gs}=0$: switch is open, no I_d flows and

$V_{gs}>0$: switch is closed, I_d flows (and more current I_d flows as V_{gs} increases)

In Fig. 17, the two operating extremes are overlaid on top of an ideal switch characteristic.

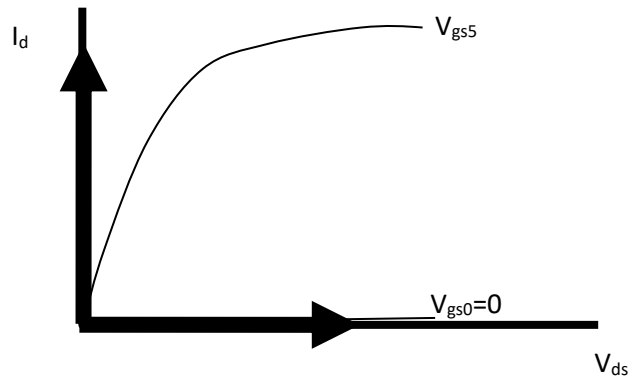


Fig. 17

MOSFETs have power handling capabilities up to only 200-300 kW, rather low. But they have switching speeds up to 1 MHz, considered to be extremely fast.

4.3 Thyristors

There are a number of different kinds of thyristors, including the silicon controlled rectifier (SCR), the bidirectional switch (Triac), and the gate turn-off thyristor (typically referred to as the GTO). We will focus on the SCR in these notes.

We first recall the operation of a diode, which is a two-terminal device having an anode (A) and a cathode (K), as shown in Fig. 18.

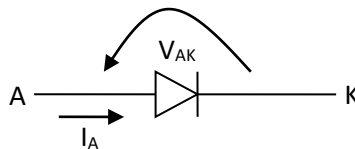


Fig. 18

We recall that the diode is also a switch, whereby the device is

- open (“off” or not conducting) when it is reversed-biased ($V_{AK} \leq 0$), and
- closed (“on”, or conducting) when it is forward-biased ($V_{AK} > 0$).

The SCR is a three terminal diode, the anode (A), cathode (K) and the gate (G), as shown in Fig. 19.

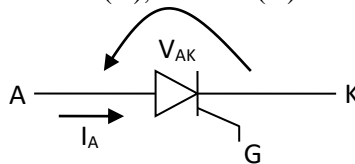


Fig. 19

This device is exactly like the diode in that it is

- open (“off” or not conducting) when it is reversed-biased ($V_{AK} \leq 0$).

However, it differs from the diode in that it is

- closed (“on”, or conducting) when it is forward-biased ($V_{AK} > 0$) AND when the gate is pulsed with a current i_G .

Thus, whereas the diode requires only forward-biasing to turn on, the SCR required forward biasing AND a gate current pulse. This means the SCR can be thought of as a *controlled diode*, where the control signal is the gate current i_G .

Although the gate current is required to turn on the SCR, it is not required that it continue in order to maintain the conducting (“on”) status. If the SCR is pulsed while it is forward-biased, then the SCR will turn “on” and remain “on” until the device is reversed biased, just like the diode. This means the gate current can be used to control when the SCR will turn on, but it cannot be used to control when the SCR turns off.

The actual characteristic of an SCR is shown in Fig. 20, which illustrates

- The forward breakover voltage V_{FO} , which is the forward-biased voltage necessary to cause conduction without the presence of a gate pulse ($i_G = 0$);
- The device conducts for lower and lower forward bias voltages V_{AK} with larger and larger gate pulses i_G ;
- Like the diode, there is a reverse bias breakdown voltage V_R which, if reached, will cause the device to be destroyed.

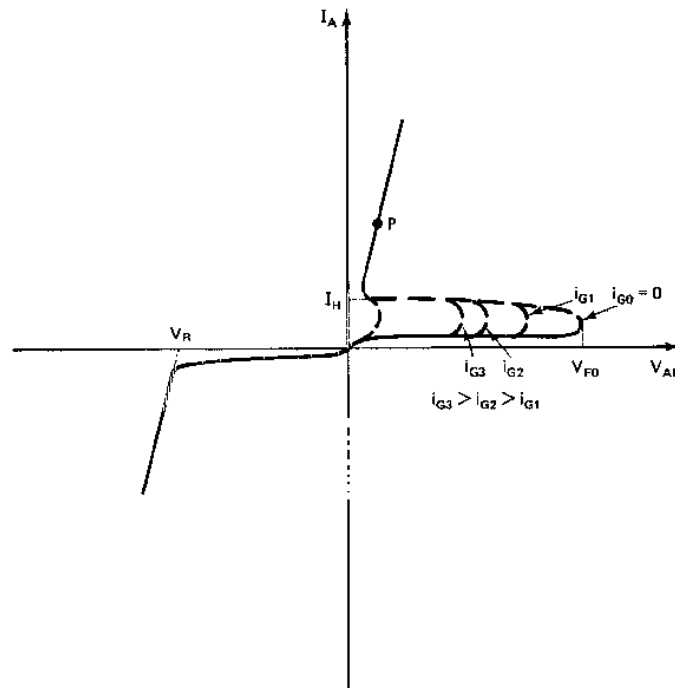


Fig. 20

SCRs have power handling capabilities up to the 20 MW range, very high, but are considered slow in that their maximum switching speed is less than 1kHz.

4.4 IGBTs

All devices described so far are referred to as single-component devices, i.e., they are comprised of a single solid-state device. The insulated gate bipolar transistor (IGBT) is different in that it is a *hybrid device* which is a device comprised of two or more solid state devices. Specifically, the IGBT combines a MOSFET with a BJT as illustrated in Fig. 21.

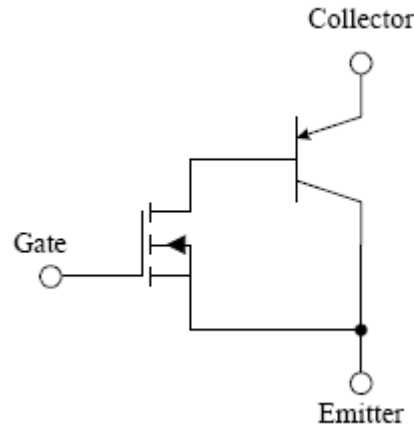


Fig. 21

The symbol for the IGBT is given in Fig. 22 together with the operating characteristic.

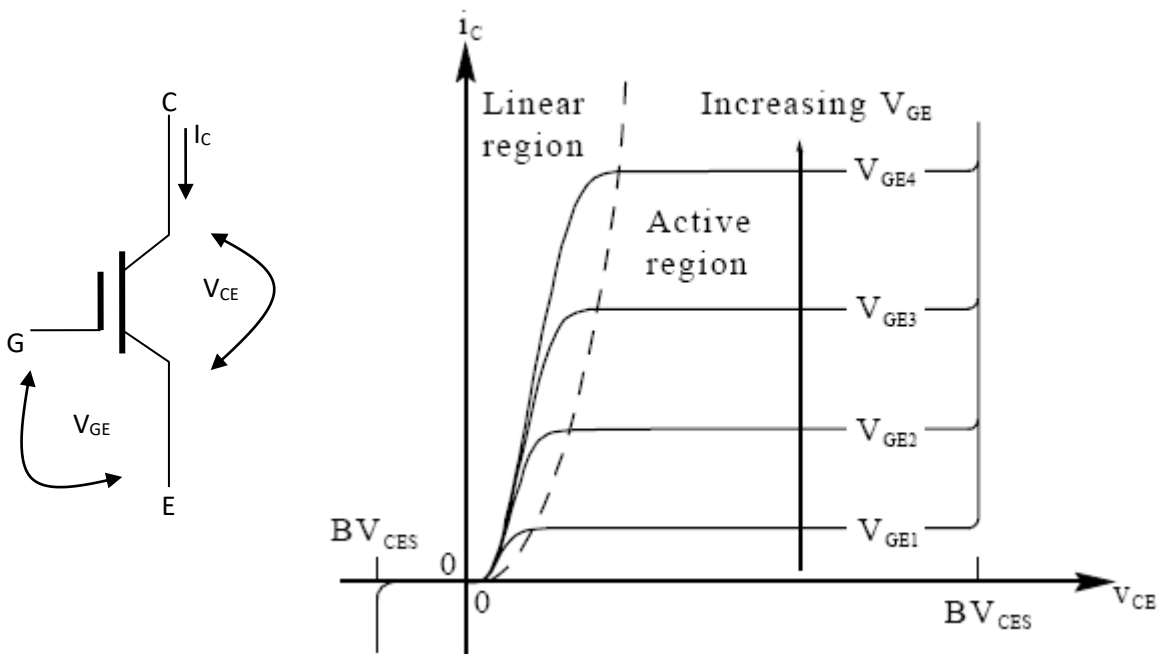


Fig. 22

IGBTs have power handling capabilities similar to BJTs, up to about 1 MW, but are capable of somewhat faster switching speeds up to 100 kHz.

4.5 Device ratings

Key distinguishing characteristics between power electronic devices are the speed at which they can switch, measured in Hz, and their power handling capabilities, which are a function of their voltage and current ratings. We have provided numerical ranges associated with these attributes for each device discussed so far. Figure 23 [] provides an effective way to compare some of these different devices in these terms.

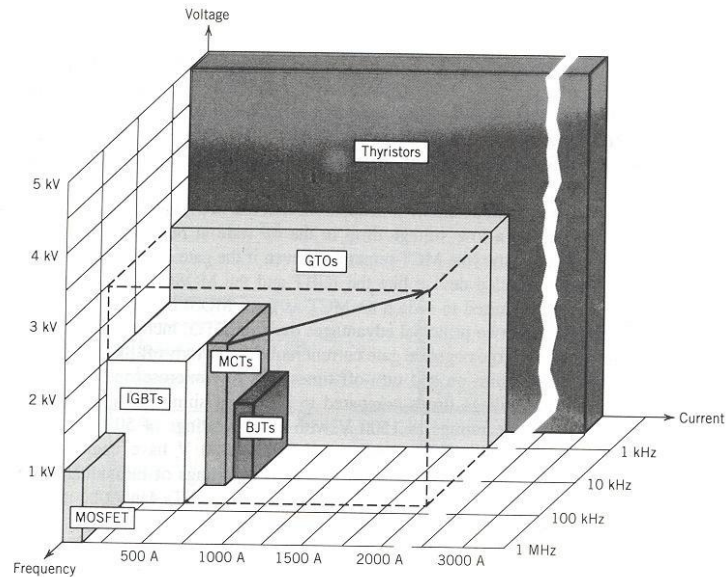


Fig. 23

The switching time is comprised of the turn-on time and the turn-off time. The turn-on time, t_{on} , is the interval between applying the triggering gate pulse and device turn-on. The turn-off time, t_q , is the time required after forward current has ceased before forward voltage may again be applied without turn-on. The maximum switching frequency is then given by $1/(t_{on}+t_q)$.

There are some other device ratings of importance, including the following:

- Voltage breakdown: This is the maximum reverse bias voltage that can be applied on an “off-state” beyond which the device breaks down and is damaged.
- Current rating: This is the maximum current the device can carry beyond which excessive heating within the device destroys it.
- Maximum di/dt : Some time is necessary during device turn-on for the current to spread uniformly across the junction, and if di/dt is too large, the current flows in too small a region of the junction, causing high current density, excessive localized heating (a hot spot), and device failure.
- Maximum dv/dt : Excessive dv/dt causes a device to turn off.

4.5.1 Limiting di/dt

4.5.2 Limiting dv/dt

5.0 Power electronic converters

We are well aware that our electric energy is delivered to us via AC systems. However, there are some DC applications, including, for example, DC motors, where we must convert AC into DC in order to supply these devices from the AC grid. There are also DC sources, including, for example, solar cells and wind turbines with DC generators, where we must convert DC to AC in order to integrate these devices into the AC grid. There are also DC transmission lines that are embedded within the AC grid which require the AC to be converted to DC at the sending end and the DC to be converted back to AC at the receiving end.

Finally, there are control applications where it is useful to convert AC to AC in order to exert control over a device. The control may be in terms of voltage, frequency, or both. A light dimmer is a very common device which converts AC to AC for control of the power that is supplied to a light bulb, thus varying its luminosity. A device which does both is called the cycloconverter, used to control motors which convert rotational motion to linear motion (so-called traction motors), as is common in rail applications. The power electronic application of interest to us here is for AC to AC control of the frequency of the induction motor rotor currents. It is illustrated in Fig. 9.

In general, power electronic circuits which convert from one power type to another are called converters. There are other names used for specific kinds of converters, as follows:

- AC to DC: rectifiers
- DC to AC: inverters
- DC to DC: choppers (also switching regulators)
- AC to AC: converters (also voltage controllers, frequency changers, or cycloconverters)

We will focus on the AC to DC rectifiers in what follows and then show how study each of these in what follows.

5.1 AC to DC

Half-wave rectifier:

A simple diode half-wave rectifier consists of an alternating voltage source in series with a diode and a resistor as shown in Fig. 24a. During the positive half cycle ($0 \leq \omega t \leq \pi$), the diode conducts and the current flows through the load resistance R. During the negative half-cycle ($\pi \leq \omega t \leq 2\pi$), the diode is off and acts like an open switch. Figure 24b shows the resulting waveforms for a sinusoidal input voltage source of $v = V_m \sin(\omega t)$.

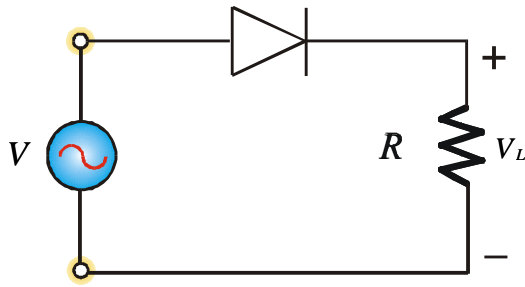


Fig. 24a: Half-Wave Rectifier Circuit

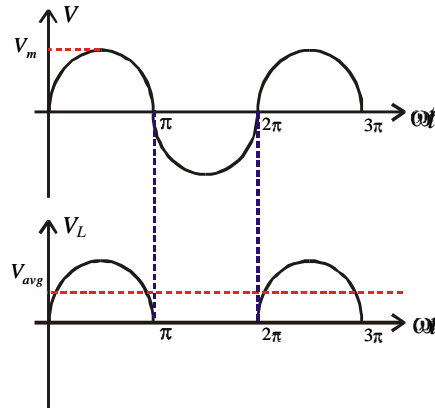


Fig. 24b: Input & Load Voltage Waveforms

The average value of a periodic waveform $x(t)$, of period T , is

$$X_{avg} = \frac{1}{T} \int_0^T x(t) dt \quad (8)$$

The average value of the voltage across the load is the DC component of the voltage and is given by:

$$V_{avg} = \frac{1}{2\pi} \int_0^\pi V_m \sin(\omega t) d(\omega t) = \frac{V_m}{\pi} \quad (9)$$

where $T = 2\pi$ but we need only integrate to π because the function is zero between π and 2π . The average value of current for the circuit of Fig. 24a is then given by

$$I_{avg} = \frac{V_{avg}}{R} = \frac{V_m}{\pi R} \quad (10)$$

The “DC power” is the power delivered to the load if the average voltage is applied across it, given by

$$P_{DC} = V_{avg} I_{avg} = \frac{V_m^2}{\pi^2 R} \quad (11)$$

However, the “DC power” is not the same as the average power. The average power is the average value of the product of instantaneous voltage $v(t)$ and instantaneous current $i(t)$, that is:

$$P_{avg} = \frac{1}{T} \int_0^T v(t) i(t) dt \quad (12)$$

The average power may be obtained by taking the product of the RMS voltage and current. For a voltage or current having a purely sinusoidal waveform, the RMS value will be 0.707 multiplied by the peak value. For a voltage or current having a non-sinusoidal waveform, the RMS value must be obtained by taking the root-mean square of the waveform over one period.

For the half wave rectifier circuit of Fig. 24a, the RMS value of the voltage across the load is

$$V_{rms} = \sqrt{\frac{1}{2\pi} \int_0^{\pi} [V_m \sin(\omega t)]^2 d(\omega t)} = \frac{V_m}{2} \quad (13)$$

The RMS current is then given by

$$I_{rms} = \frac{V_{rms}}{R} = \frac{V_m}{2R} \quad (14)$$

The average power is then given by

$$P_{avg} = V_{rms} I_{rms} = \frac{V_m^2}{4R} \quad (15)$$

We observe that the average power is greater than the “DC power” for a purely resistive circuit by a factor of

$$\frac{P_{avg}}{P_{DC}} = \frac{\frac{V_m^2}{4R}}{\frac{V_m^2}{\pi^2 R}} = \frac{\pi^2}{4} = 2.4674 \quad (16)$$

Therefore, computing power must be done with RMS quantities. Although DC quantities for voltages and currents are often obtained for power electronic circuits, their use for power calculations should always be seen to be approximations at best [6, pg. 40]. Two other ways to compute power that are of interest when either one or both waveforms are nonsinusoidal include [6, pp. 37-40] (a) taking the average of the product of instantaneous voltage and current; and (b) taking a Fourier series of voltage and current and then adding products of like harmonics.

Controlled Half-wave rectifier:

A simple form of a controlled half-wave rectifier feeding a resistive load, such as an electric heater or incandescent lamp, is shown in Fig. 25a. If the input source $v_i(\omega t) = V_m \sin(\omega t)$ is as drawn in Fig. 25b, the corresponding output voltage and the resulting current wave are as indicated in Fig. 25c for a particular triggering (firing) angle α . The anode-cathode voltage across the thyristor is depicted in Fig. 25d. The triggering current pulse of suitable magnitude and duration required to turn on the SCR at $\omega t = \alpha$ is shown in Figure 25e. If $\alpha = 0$, we realize an uncontrolled half-wave rectifier employing a diode. For this scheme, the average value of the output voltage V_{dc} is:

$$\begin{aligned}
 V_{dc} &\equiv \frac{1}{2\pi} \int_{\alpha}^{\pi} V_m \sin(\omega t) d(\omega t) \\
 &= \frac{V_m}{2\pi} [-\cos \omega t]_{\alpha}^{\pi} \\
 &= \frac{V_m}{2\pi} [1 + \cos \alpha]
 \end{aligned}
 \tag{17}$$

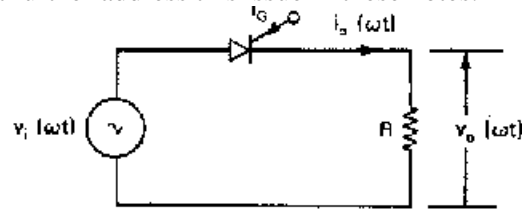
and the corresponding current I_{dc} is given by

$$I_{dc} = \frac{V_{dc}}{R} = \frac{V_m}{2\pi R} [1 + \cos \alpha]
 \tag{18}$$

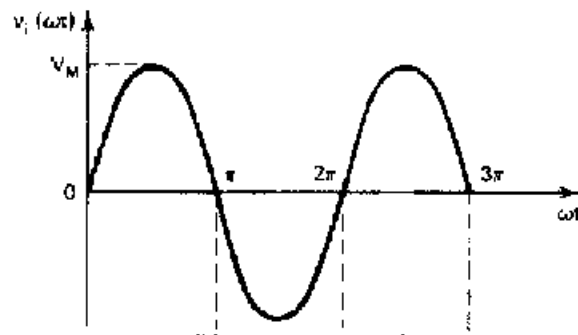
If $\alpha = 0$, then $V_{dc} = V_m/\pi$ and this value goes to zero if $\alpha = \pi$. Therefore, by varying α from 0 to π , one can completely vary the dc output voltage from zero to the maximum value of (V_m/π) . The corresponding power dissipated in R will be

$$P_{dc} = \frac{V_{dc}^2}{R} = I_{dc}^2 R = \frac{V_m^2}{4\pi^2 R} [1 + \cos \alpha]^2
 \tag{19}$$

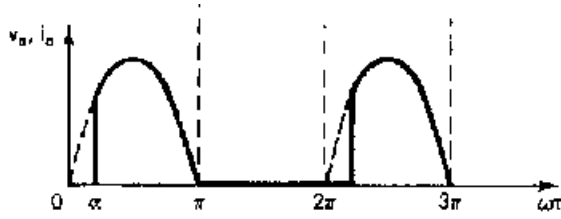
One important observation we can make at this point, with respect to controlled power electronics circuits, is the nonsinusoidal nature of resulting waveforms as shown in Figure 25c. The output voltage and current in this circuit contains various harmonics that can be determined by performing a Fourier series analysis. We will not further address this issue in these notes.



(a) Circuit diagram



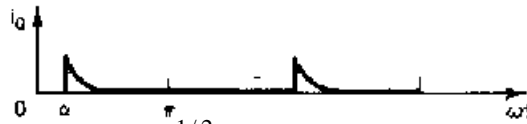
(b) Input source waveform



(c) Output voltage and current waveforms



(d) Thyristor voltage waveform



$$V_{\text{rms}} \equiv \left[\frac{1}{2\pi} \int_{\alpha}^{\pi} (V_m \sin(\omega t))^2 d(\omega t) \right]^{1/2}$$

Figure 25: Single-phase half-wave controlled rectifier

The RMS value of the output voltage, is given by:

$$= \left[\frac{1}{2\pi} \int_{\alpha}^{\pi} V_m^2 \sin^2(\omega t) d(\omega t) \right]^{1/2} = \left[\frac{1}{2\pi} \int_{\alpha}^{\pi} V_m^2 \frac{1 - \cos(2\omega t)}{2} d(\omega t) \right]^{1/2}$$

$$= \left[\frac{V_m^2}{4\pi} \int_{\alpha}^{\pi} 1 - \cos(2\omega t) d(\omega t) \right]^{1/2} = \frac{V_m}{2\sqrt{\pi}} \left[\left(\omega t - \frac{\sin(\omega t)}{2} \right) \right]_{\alpha}^{\pi}$$

$$= \frac{V_m}{2\sqrt{\pi}} \left[(\alpha - \pi) - \frac{\sin(\pi) - \sin(\alpha)}{2} \right]^{1/2} = \frac{V_m}{2\sqrt{\pi}} \left[(\alpha - \pi) + \frac{\sin(\alpha)}{2} \right]^{1/2}$$

Consequently,

$$I_{\text{rms}} = \frac{V_{\text{rms}}}{R} = \frac{V_m}{2\sqrt{\pi}R} \left[(\pi - \alpha) + \frac{\sin 2\alpha}{2} \right]^{1/2}$$

(20)

(21)

We now define a measure called *ripple factor* of all ac components of the smoothness of the output voltage.

$$r(\%) \equiv \frac{\sqrt{V_{rms}^2 - V_{dc}^2}}{V_{dc}} \times 100 \quad (22)$$

This can be shown to reduce to:

$$r = \left[\frac{V_{rms}^2}{V_{dc}^2} - 1 \right]^{1/2} \times 100 = \frac{\sqrt{V_{rms}^2 - V_{dc}^2}}{V_{dc}} \times 100 \quad (23)$$

Full wave rectifier:

The full wave rectifier is described in Module PE1 of your notes.

Three phase rectifier:

The single-phase, full-wave bridge scheme can be extended to accommodate a three-phase input source. Most popular and versatile is the 6-pulse converter, or controlled rectifier. Prior to the invention of thyristors, mercury arc rectifiers were employed to realize controlled rectification. The well-known Pacific ± 500 kV, HVDC transmission line linking the northwest region at Celilo, Oregon, to Sylmar, near Los Angeles in the southwest region, adopted the mercury arc rectifiers. We will explore this important application later in this section after gaining an understanding of this converter scheme.

The circuit of Fig. 25 employs a Y-connected, three-phase source $v_i(\omega t)$, delivering dc output $v_o(\omega t)$ to resistive load through a thyristor bridge consisting of six controlled switches; hence it is called a 6-pulse converter.

The operation of the scheme can be understood based on the following observations:

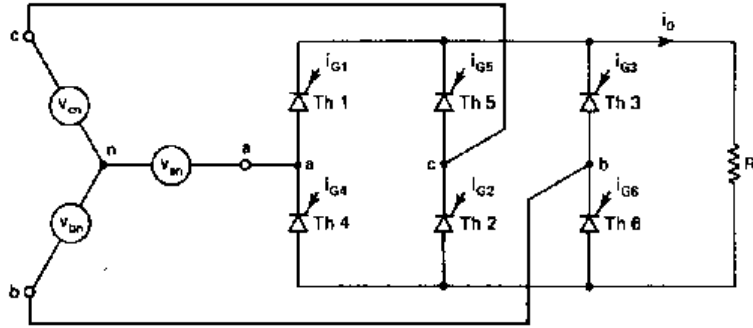
1. Exactly two SCRs are conducting at any moment, as can be seen from the bottom of Fig. 26c.
 - One SCR is fired at $\alpha = \omega t$ and then left on for 60° , after which an SCR is fired every 60° thereafter.
 - We turn on the pair of SCRs that give the most positive line-to-line voltage. We can determine the SCR pair that should be on by (a) identifying the most positive line-to-line voltage; (b) inspecting the circuit and identifying how to place the most positive line-to-line voltage across the load.
2. Thyristors turn off when they become reversed biased. This occurs whenever the voltage applied at their cathode exceeds the voltage applied at their anode.

For the time period $\omega t = 0$ to $\pi/3$,

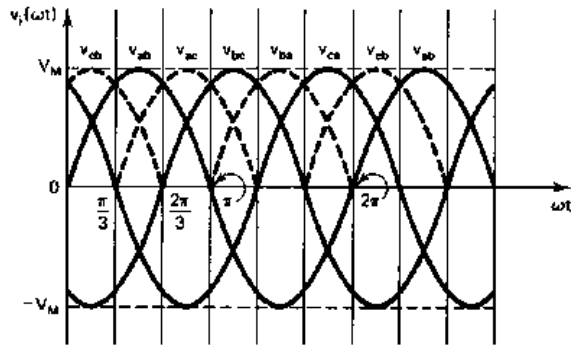
- v_{cb} is the most positive voltage relative to other line-to-line voltages;
- Th 5, 6 conduct if suitable pulses are applied, or are already applied, to their respective gates;
- at the end of the time period, at $\omega t = \pi/3$, we turn on Th 1 to apply v_{ab} across the load;
- Although Th5 is on at $\omega t = \pi/3$, v_{ab} goes higher than v_{cb} at that moment, which reverse biases Th 5, and it commutates (turns off).

For the time period $\omega t = \pi/3$ to $2\pi/3$,

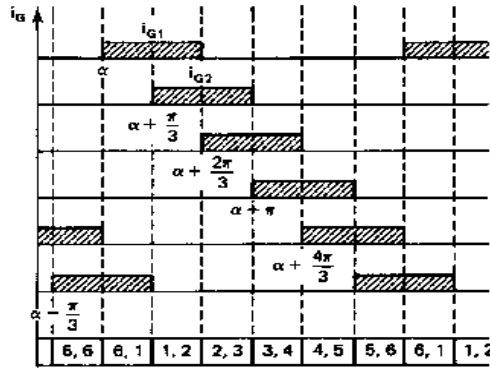
- v_{ab} is the most positive voltage relative to other line-to-line voltages;
- Th 1, 6 conduct if suitable pulses are applied, or are already applied, to their respective gates;
- at the end of the time period, at $\omega t = 2\pi/3$, we turn on Th 2 to apply v_{ac} across the load;
- Although Th6 is on at $\omega t = 2\pi/3$, v_{ac} goes higher than v_{ab} at that moment, which reverse biases Th 6, and it commutates (turns off).



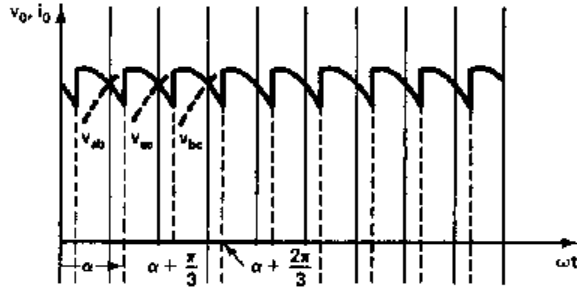
(a) Circuit schematic



(b) Balanced, three-phase input source



(c) Gate pulses and thyristor conduction sequence



(d) Output signal waveforms

Fig. 26: Three-phase, full-wave controlled rectifier scheme

A close observation of v_o clearly shows that its fundamental frequency of variation is six times that of the input source. Therefore, the harmonic of the output voltage will be multiple orders of 6, a clear advantage with a polyphase source. In addition, the ripple in v_o will also be much lower than in the single-phase scheme we discussed earlier in this chapter. Consequently, we can obtain higher quality (or less ripple) output.

The average value of v_o is $V_{dc} = \frac{3}{\pi} \int_{\alpha+(\pi/3)}^{\alpha+(2\pi/3)} v_o(\omega t) d(\omega t) = \frac{3}{\pi} \int_{\alpha+(\pi/3)}^{\alpha+(2\pi/3)} v_{ab}(\omega t) d(\omega t)$

$$= \frac{3}{\pi} \int_{\alpha+(\pi/3)}^{\alpha+(2\pi/3)} V_M \sin(\omega t) d(\omega t) = \frac{3V_M}{\pi} \cos \alpha \quad (24)$$

where V_M is the maximum line-to-line voltage. In a similar manner, the rms value of the load voltage is:

$$V_{rms} = \left[\frac{3}{\pi} \int_{\alpha+(\pi/3)}^{\alpha+(2\pi/3)} v_o^2 d(\omega t) \right]^{1/2} = V_M \left[\frac{1}{2} + \frac{\cos(2\alpha)}{4\pi} \right]^{1/2} \quad (25)$$

The approach taken in the converter for the DFIG is to use what is called a slip energy recovery circuit, also known as a static Scherbius circuit. Essentially, it connects two three-phase rectifier circuits in series, as illustrated below [6, pp. 200-209]. Another excellent treatment is provided in [7], and some other worthwhile references to check include [8, 9, 10].

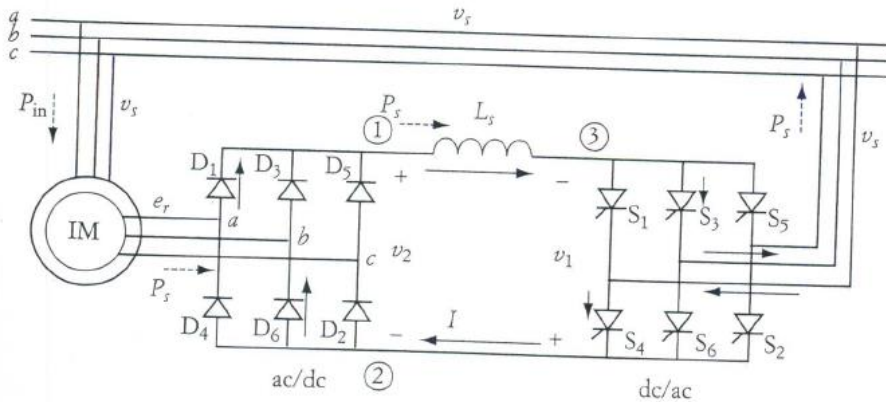


Fig. 27 [6]

Some other issues to address:

- Operation of the DC to AC link, PWM.
- Ability for power to flow through the converter in both directions.
- Functionality of the DC link, with inductor, and with capacitor.
- Definition of the voltage source converter.

5.2 DC to AC

5.3 DC to DC

5.4 AC to AC

-
- [1] T. Thiringer, A. Petersson and T. Petru, “Grid Disturbance Response of Wind Turbines Equipped with Induction Generator and Doubly-Fed Induction Generator,” 2003.
- [2] M. El Sharkawi, “Electric Energy: An Introduction,” second edition, CRC Press, 2008.
- [3] S. Soter and R. Wegener, “Development of Induction Machines in Wind Power Technology,” available at http://www-mal.e-technik.uni-dortmund.de/paper/upload/paper_71.pdf.
- [4] B. Fox, et al., “Wind Power Integration: Connection and System Operational Aspects,” Institution of Engineering and Technology, UK, 2007, pp. 73-75, available at http://books.google.com/books?id=LTuo24RfTGoC&pg=PR6&lpg=PR6&dq=%22Induction+generator%22+%22fixed-speed%22+%22energy+extraction%22&source=bl&ots=H6HqFRz2fi&sig=ILiL_n-bEoOMJyOjTW7bzWwebGI&hl=en&ei=6MLVS7zPDsO88gbQkqHIDw&sa=X&oi=book_result&ct=result&resnum=4&ved=0CBgQ6AEwAzgU#v=onepage&q=%22Induction%20generator%22%20%22fixed-speed%22%20%22energy%20extraction%22&f=false.
- [5] M. Rashid, “Power electronics: Circuits, Devices, and Applications,” second edition, Prentice-Hall, 1993.
- [6] M. El-Sharkawi, “Fundamentals of Electric Drives,” Brooks/Cole Publishing, 2000.
- [7] I. Boldea, “Variable Speed Generators,” Taylor & Francis, 2006.
- [8] I. Boldea and S. Nasar, “The Induction Machine Handbook,” CRC Press, 2000.
- [9] S. Heier, “Grid Integration of Wind Energy Conversion Systems,” Wiley, 1998.
- [10] M. Stiebler, “Wind Energy Systems for Electric Power Generation,” Springer, 2008.